Progress In Electromagnetics Research Letters, Vol. 105, 103–109, 2022

Efficient Broadband Power Amplifier Using Klopfenstein Taper as Output Matching Network

Duo-Wei Liu[1], Fei Cheng[1, *], Chao Gu[2], and Kama Huang[1]

Abstract—An efficient 0.6–4.2 GHz GaN-HEMT power amplifier based on Klopfenstein taper is proposed in this letter. A method based on source-pull/load-pull simulation has been used to find the optimum source and load impedances across the broad band. Then the Klopfenstein taper is studied and adopted for the output matching circuit design to achieve broadband performance. The measured results show that our proposed power amplifier has a fractional bandwidth of 150%, with saturated output power ranging from 39.45 to 42.32 dBm, power added efficiency from 45.1% to 64.8%, and over 9 dB gain at the whole working band of 0.6–4.2 GHz. The fabricated power amplifier can cover most of the wireless communication frequency bands.

1. INTRODUCTION

With the development of wireless communication technology, more and more frequency bands are used, and broadband capabilities are required for radiofrequency devices. Especially, the modern digital controlled software radio system makes the transmitter with multi-octave band operation possible [1]. As a critical component of the transmitter, power amplifier (PA) determines its bandwidth, efficiency, and communication distance. Thus, broadband PA has attracted great attention in recent years [2–6].

It is really a challenge to meet the need of both high efficiency and broadband working of the PA. To achieve this goal, the output network must satisfy wideband matching requirement. In [2], a branch line coupler was employed in the output matching network (OMN) of the PA. By appropriately selecting the impedance conditions of the output port, the branch line coupler can not only transform the fundamental impedance, but also control the harmonic impedance. In [3], a simultaneous search of the impedance space and possible matching networks via particle swarm optimization can identify the design solution. The prototype amplifier demonstrates an outstanding gain of 12.8–14.9 dB, output power greater than 40 dBm, and efficiency between 51% and 70% over a target frequency range of 2.4–4.6 GHz. In [4], Wright et al. proved that Class-J mode had the potential to realize a PA with a bandwidth from 1.35 to 2.25 GHz and over 60% drain efficiency. In [5], an extended continuous mode voltage equation was presented, and the second harmonic clipping contours were integrated into the traditional design flow. An 8.5 W PA with efficiency over 60% and a bandwidth of 1–2.9 GHz was realized using this method. In [6], an extended Chebyshev function was proposed to adapt the matching condition of the PA by introducing a new factor. A set of impedance functions can be directly calculated along with the variation of a new variable, and the first element extracted from the functions is distributed in a wide range. To achieve better performances, the real frequency technique is applied to adjust the harmonic impedances.

In this work, a broadband high efficiency PA is designed and fabricated. A Klopfenstein taper which can realize real-to-real transformation is employed to achieve wideband matching for the OMN.

Received 2 March 2022, Accepted 20 July 2022, Scheduled 1 August 2022
* Corresponding author: Fei Cheng (chengfei@scu.edu.cn).
[1] College of Electronics and Information Engineering, Sichuan University, Chengdu 610065, People's Republic of China. [2] Centre for Wireless Innovation, ECIT Institute, Queens University Belfast, Belfast, BT3 9DT, UK.

The design principles for the high efficiency PA using this structure are given. Under the continuous-wave excitation, the measured PAE of the fabricated PA ranges from 45.1% to 64.8%, and the saturated output power exceeds 39.45 dBm over the operating frequency of 0.6–4.2 GHz.

2. OPTIMAL OUTPUT IMPEDANCE REGION ANALYSIS

The CGH40010F GaN HEMT from Cree Inc. with drain bias voltage of 28 V and gate voltage of −2.7 V is adopted in this design. In order to design the OMN, the optimal output impedance region is analyzed firstly. Fig. 1 shows the simulated constant output power contours, constant efficiency contours, and their overlapping area at 0.5–4.5 GHz which are obtained from load-pull simulation in Keysight Pathwave 2020. As shown in Fig. 1, with the increase of frequency, the constant output power contours and constant efficiency contours both move counterclockwise from the upper left to the lower left on the Smith chart. At low frequencies, both the constant power contours and constant PAE contours would cover a large impedance area. With the increase of frequency, the region of those curves tends to converge. The optimal power impedance point and optimal efficiency impedance point are not coincident, so there is a trade-off area between them. Fig. 1(c) shows their overlapping area in which the output power is larger than 41 dBm, and the PAE is higher than 50%. In Fig. 1(c), 18 Ω is inside all the contours. Thus, it is chosen as the output impedance of the PA to perform the real-to-real

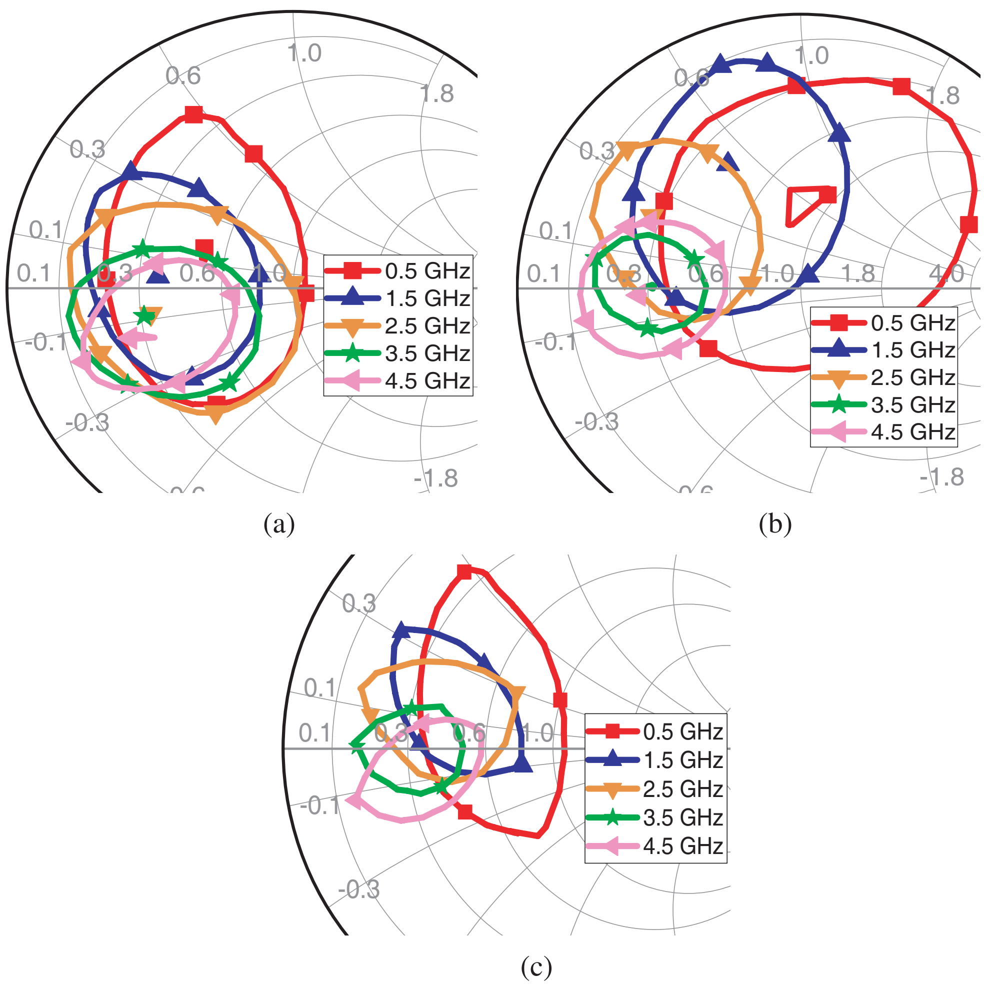

Figure 1. Constant output power contours, constant PAE contours and their overlapping area at different frequencies. (a) Constant output power contours ($P_{out} > 41$ dBm), (b) constant PAE contours (PAE > 50%). (c) Their overlapping part ($P_{out} > 41$ dBm and PAE > 50%).

transformation using the Klopfenstein taper.

3. OUTPUT MATCHING NETWORK DESIGN

The Klopfenstein taper is adopted in the OMN design which can perform real-to-real impedance transformation, shown in Fig. 2(a). It is derived from a stepped Chebyshev transformer when the number of transmission line sections of Chebyshev transformer increases to infinity. For a given length, Klopfenstein taper is optimal in terms of minimum reflection coefficient in the passband compared with Chebyshev taper [7]. In other words, the length of Klopfenstein impedance transformer is shorter than that of Chebyshev transformer with the same reflection coefficient.

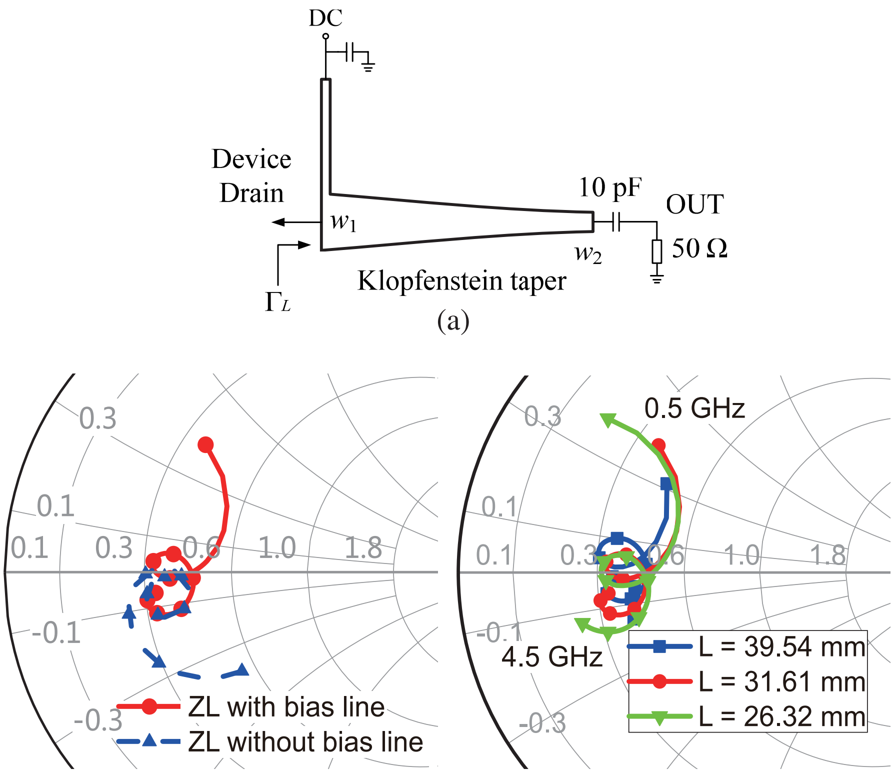

Figure 2. Proposed OMN and the simulated results. (a) Proposed OMN. (b) Simulated ZL with and without the bias line. (c) Simulated ZL of the Klopfenstein taper with different length.

The logarithm of the characteristic impedance variation for the Klopfenstein taper is given by [7]

$$\ln Z(z) = \frac{1}{2}\ln Z_0 Z_L + \frac{\Gamma_0}{\cosh A} A^2 \varphi(2z/L - 1, A) \quad 0 \le z \le L \tag{1}$$

where Γ_0 is the reflection coefficient at zero frequency with $\Gamma_0 = (1/2)\ln(Z_L/Z_0)$; A is defined as $A = \cosh^{-1}(\Gamma_0/\Gamma_m)$ where Γ_m is the maximum ripple in the passband; and function $\varphi(x, A)$ is defined as

$$\varphi(x, A) = -\varphi(-x, A) = \int_0^x \frac{I_1\left(A\sqrt{1-y^2}\right)}{A\sqrt{1-y^2}} dy \quad |x| \le 1 \tag{2}$$

where $I_1(x)$ is the modified Bessel function. The reflection coefficient is given by

$$\Gamma(\theta) = \Gamma_0 e^{-j\beta L} \frac{\cos\sqrt{(\beta L)^2 - A^2}}{\cosh A} \quad \beta L > A \tag{3}$$

In our design, $Z_0 = 50\,\Omega$ and $Z_L = 18\,\Omega$. We can get $\Gamma_0 = 0.51$. Γ_m is 0.1 which means $|S_{11}| = -20\,\text{dB}$. Thus, we can get $A = 2.31$. Then, the characteristic impedance of each section of the Klopfenstein taper can be decided by (1) with different lengths of the Klopfenstein taper.

In Fig. 2(a), a high characteristic impedance transmission line parallel with a capacitor is used to provide DC for the transistor which is required to isolate the DC path and RF path over a wide bandwidth. This bias line also plays an important role in the matching circuit which acts as reactance in parallel at RF frequencies. Fig. 2(b) shows the locus of the input impedance with and without the bias line on the Smith chart. As shown, the impedance locus without the bias line is in the lower semicircle of the Smith chart. When a bias line is connected, the impedance locus moves to match the optimal output impedance of the transistor. So the PA can achieve high power and high efficiency over multiple octaves.

The characteristic impedance of each end of the Klopfenstein taper is fixed to 18 and $50\,\Omega$, respectively. By changing the length of the Klopfenstein taper, the bandwidth of the OMN can be changed. Fig. 2(c) compares the simulated locus of the input impedance of the Klopfenstein taper with different lengths. As shown, when the length is 26.32 mm, the impedance at lower frequencies is outside the optimal impedance region in Fig. 1(c). When the length is 39.54 and 31.61 mm, the impedance is inside the optimal impedance region in Fig. 1(c). To reduce the PA size, 31.61 mm is chosen as the length of the Klopfenstein taper.

4. INPUT MATCHING NETWORK DESIGN

After the output matching network is defined, the input matching network (IMN) is designed to match the input impedance. Fig. 3 shows schematic of the input matching network and the input impedance of the transistor obtained from source-pull simulation in Keysight PathWave 2020. In Fig. 3, with the increase of frequency, the locus of the optimal input impedance turns counterclockwise from the upper

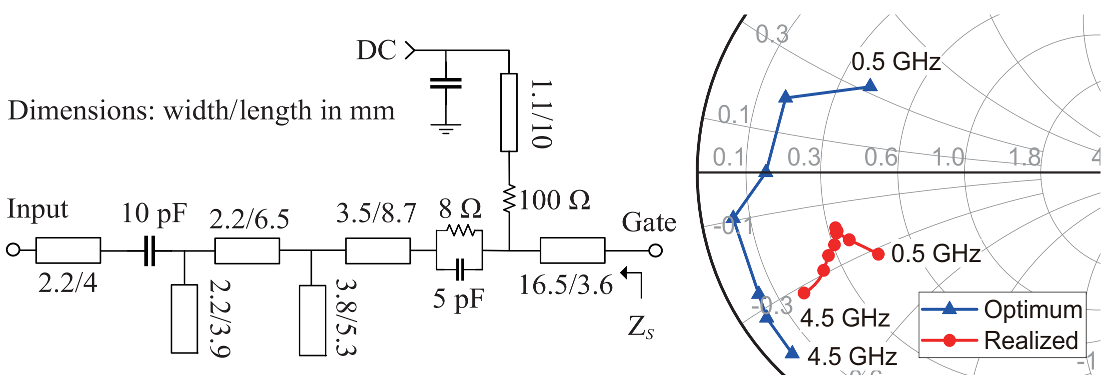

Figure 3. Schematic of the input matching network as well as optimum and realized source impedances.

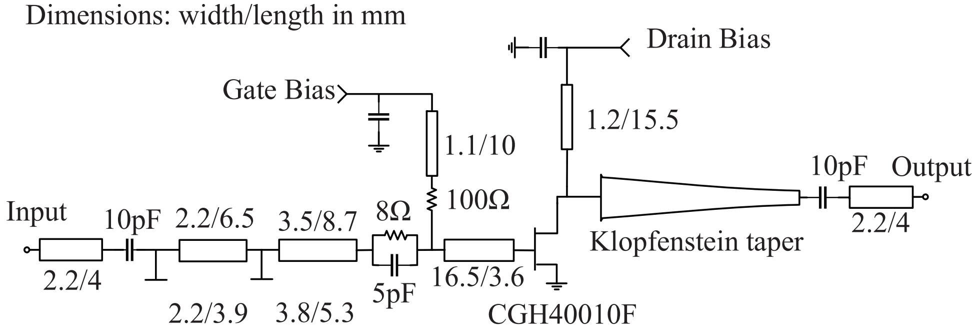

Figure 4. Schematic of the proposed PA.

half of Smith chart to the lower half part, and the real part of impedance becomes very small at high frequencies which is around 4 Ω. It is difficult to design a microstrip network to match such a low real-part impedance to keep the gain of the amplifier high. The parallel RC circuit is series-connected to the IMN to make the device stable at low frequencies while maintaining the gain at high frequencies.

5. IMPLEMENTATION AND MEASUREMENT RESULTS

The circuit diagram of the designed PA is depicted in Fig. 4. Fig. 5 shows a photograph of the proposed PA which is fabricated on a 0.8 mm F4B substrate with a size of 80 mm × 38 mm (F4B: $\varepsilon_r = 2.6$, loss tangent = 0.002, metal thickness = 0.018 mm). The simulated and measured results of the proposed PA are shown in Fig. 6. In Fig. 6(a), the simulated results show that the proposed PA delivers saturated output power higher than 40 dBm across 0.6–4.2 GHz while the gain ranges between 10 and 15 dB with PAE exceeding 50%. The measured saturated output power agrees well with the simulated one which ranges from 9.5 to 16.2 W from 0.6 to 4.2 GHz. The measured PAE agrees with the simulated one at low frequencies, and it is slightly lower than the simulated one when the frequency is higher than 3 GHz. It is guessed that the transistor model is not very accurate at high frequencies. However, the overall trend is relatively consistent. In Fig. 6(b), the PA reaches its highest gain of 15.7 dB at 0.6 GHz with the saturated output power of 39.5 dBm and PAE of 62.4%. Table 1 compares the broadband power amplifier performance in the literatures and that in this work. As can be seen, our work has a relative

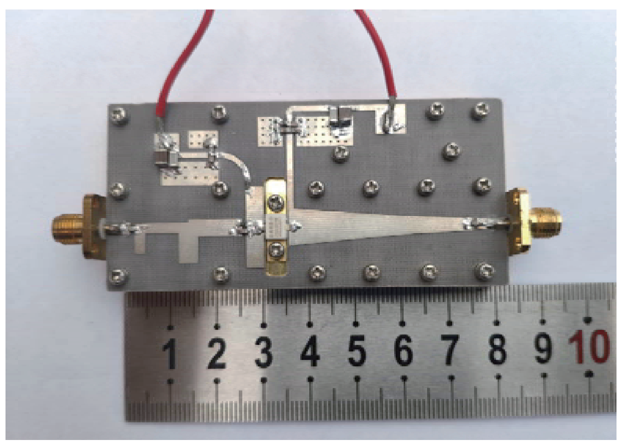

Figure 5. Photograph of the fabricated PA.

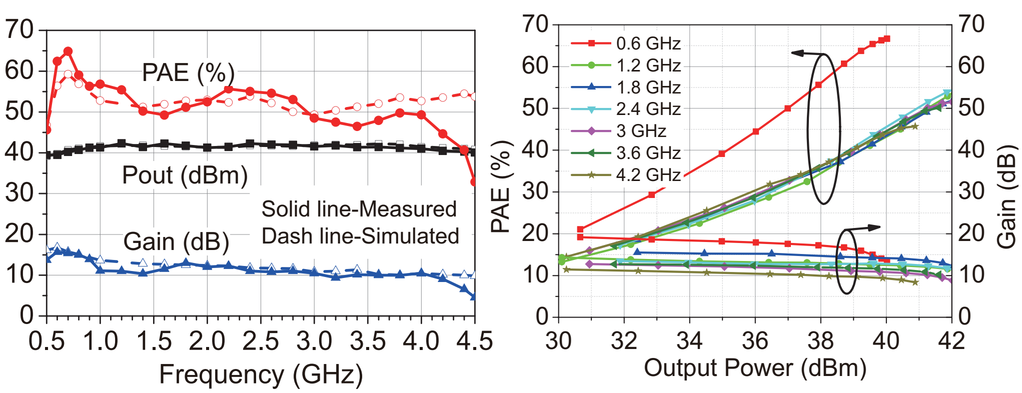

(a) (b)

Figure 6. Simulated and measured results. (a) Simulated and measured PAE, output power, and gain vs. frequency. (b) Measured PAE and gain vs. output power at different frequencies.

Table 1. Comparison with recent research on broadband PAs.

Reference	Frequency (GHz)	BW (%)	Gain (dB)	P_{out} (W)	Efficiency (%)
[2]	1.0–3.0	100	10.2–11.5	12.5–17.7	64–75 D
[3]	2.4–4.6	62.8	12.8–14.9	10–19	51–70 D
[6]	1.6–3.5	75	9.4–14.9	11.7–20.4	58–74 D
[8]	0.5–4.0	156	10.1–12.8	10–19	60–71 D
[9]	0.5–3.15	145.2	8.43–15.67	8–19.3	58–74.9 P
This work	0.6–4.2	150	9–15.7	9.5–16.2	45.1–64.8 P

D: Drain Efficiency P: Power Added Efficiency

wide fractional bandwidth compared to most of other works while the PAE is also competitive compared to those works.

6. CONCLUSION

In this letter, a broadband high efficiency PA has been presented. The Klopfenstein taper structure is synthesized by numerically aided calculation, and then the inductive reactance is introduced through the microstrip offset stub to form the output matching network of the power amplifier circuit. The input matching network provides appropriate gain compensation. To demonstrate, a PA is designed and fabricated. Large signal measurement results show 150% fractional bandwidth, output power of 39.45–42.32 dBm, and PAE of 44.6%–64.8%.

ACKNOWLEDGMENT

This work was supported in part by the National Natural Science Foundation of China (Grant No. 61801317), in part by the Sichuan Science and Technology Program: Provincial Overseas Cooperation (Grant No. 2022YFH0097), in part by the State Key Laboratory of Millimeter Waves (Grant No.K202206) and in part by the Fundamental Research Funds of Shaanxi Key Laboratory of Artificially-Structured Functional Materials and Devices (Grant number: AFMD-KFJJ-21202).

REFERENCES

1. Rawat, K., M. S. Hashmi, and F. M. Ghannouchi, "Dual-band RF circuits and components for multi-standard software defined radios," *IEEE Circuits and Systems Magazine*, Vol. 12, No. 1, 12–32, Firstquarter 2012.
2. Zhang, Z., Z. Cheng, H. Ke, and G. Liu, "A broadband high-efficiency power amplifier by using branch line coupler," *IEEE Microw. Wireless Compon. Lett.*, Vol. 30, No. 9, 880–883, Sept. 2020.
3. Poluri, N. and M. M. De Souza, "Designing a broadband amplifier without load-pull," *IEEE Microw. Wireless Compon. Lett.*, Vol. 31, No. 6, 593–596, Jun. 2021.
4. Wright, P., J. Lees, P. J. Tasker, J. Benedikt, and S. C. Cripps, "An efficient, linear, broadband class-J-mode PA realised using RF waveform engineering," *2009 IEEE MTT-S International Microwave Symposium Digest*, 653–656, 2009.
5. Canning, T., P. J. Tasker, and S. C. Cripps, "Continuous mode power amplifier design using harmonic clipping contours: Theory and practice," *IEEE Trans. Microw. Theory Techn.*, Vol. 62, No. 1, 100–110, Jan. 2014.

6. Dai, Z., S. He, J. Peng, C. Huang, W. Shi, and J. Pang, "A semianalytical matching approach for power amplifier with extended Chebyshev function and real frequency technique," *IEEE Trans. Microw. Theory Techn.*, Vol. 65, No. 10, 3892–3902, Oct. 2017.
7. Pozar, D. M., *Microwave Engineering*, Wiley, New York, 2011.
8. Zhang, Z. and Z. Cheng, "A multi-octave power amplifier based on mixed continuous modes," *IEEE Access*, Vol. 7, 178201–178208, 2019.
9. Chen, H., J.-X. Xu, Z.-H. Kong, W.-H. Chen, and X. Y. Zhang, "Broadband high-efficiency power amplifier with quasi-elliptic low-pass response," *IEEE Access*, Vol. 8, 52566–52574, 2020.